Effect of Temperature on the Supramolecular Tubular Structure in Oriented Fibers of a Poly(methacrylate) with Tapered Side Groups

Yong Ku Kwon, Sergei N. Chvalun, John Blackwell,* Virgil Percec, and James A. Heck

Department of Macromolecular Science, Case Western Reserve University, Cleveland, Ohio 44106-7202

Received May 31, 1994; Revised Manuscript Received December 12, 1994®

ABSTRACT: X-ray methods have been used to investigate the changes in structure with temperature for the supramolecular structure formed by a poly(methacrylate) with tapered side chains. The polymer is poly[2-[2-[2-[2-(methacryloyloxy)ethoxy]ethoxy]ethoxy]ethyl 3,4,5-tris[[*p*-(dodecyloxy)benzyl]oxy]benzoate]. Oriented fibers drawn from the columnar hexagonal (ϕ_h) liquid crystalline phase at ~60 °C adopt an ordered structure at room temperature, in which ordered cylindrical moieties are packed on a hexagonal lattice with $a \approx 60$ Å. The internal structure of the cylinder has an axial repeat of $c = 5.03$ Å, which contains eight monomer units based on the density. Integral half-widths for the small-angle and wide-angle maxima yield lateral crystallite widths of 820 and ≤50 Å, respectively. These data show that there is a high degree of perfection in the packing of the cylinders, but there is little or no correlation of the internal structure from one cylinder to the next. At the transition to the ϕ_h phase at ~40 °C there is a loss of order in the structure within the cylinder: all that remains are limited correlations due to stacking of the side chains along the axial direction. The separation between the stacked units increases with temperature, while the cylinder diameter decreases steadily from 60.4 Å at 39.9 °C to ~54 Å at 95 °C. These structural changes are correlated with striking changes in the dimension of the fibers with temperature. The dimensions show little change with temperature in the ordered solid state, but after passing through the transition to the ϕ_h phase there is a ~28% increase in length and ~14% decrease in width on increasing the temperature from 40 to 95 °C, just below the ϕ_h-to-isotropic transition, pointing to a progressive rearrangement of the supramolecular organization.

Introduction

In a previous paper[1] we described preliminary investigations of the structure formed by a poly(methacrylate) with bulky tapered side chains: poly[2-[2-[2-[2-(methacryloyloxy)ethoxy]ethoxy]ethoxy]ethyl 3,4,5-tris[[*p*-(dodecyloxy)benzyl]oxy]benzoate], hereafter abbreviated as 12-ABG-4EO-PMA. The chemical structure is shown below:

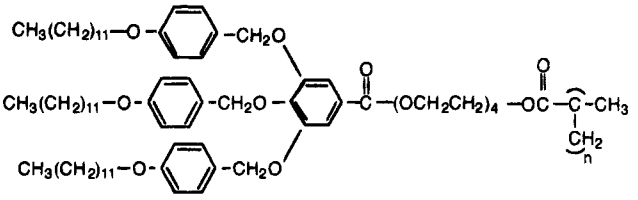

12-ABG-4EO-PMA is one of a group of polymers described by Percec *et al.*[2] that self-assemble to form supramolecular tubular architectures and generate columnar hexagonal (ϕ_h) liquid crystalline phases. The polymers have been synthesized in an effort to create self-assembling structures analogous to the rodlike viruses, such as tobacco mosaic virus.[3] The bulky tapered 3,4,5-tris[[*p*-(dodecyloxy)benzyl]oxy]benzoate (12-ABG) group mimics the shape of the protein subunits of the viral coat. 12-ABG and other tapered groups have also been used in other laboratories to design molecular[4] and supramolecular[5] liquid crystals displaying ϕ_h and other liquid crystalline phases. Alternative methods to generate self-assembling disk-like and cylindrical structures that form ϕ_h phases have also been reported.[6]

Initial studies[2a,b] showed that 12-ABG-4EO-PMA is ordered in the solid state at room temperature and undergoes a transition at approximately 47 °C to form a ϕ_h phase analogous to the structures seen for certain low molecular weight discotic liquid crystals.[7] The ϕ_h structure was identified by the observation of three small-angle maxima pointing to the existence of cylindrical assemblies packed on a hexagonal lattice with dimension $a = 57.2$ Å at 74 °C. The ϕ_h phase was stable up to approximately 100 °C, above which the polymer became isotropic. Hexagonal packing was also observed in the solid-state structure at room temperature (25 °C) but with the a dimension increased to 60 Å.

In an effort to investigate the internal structure of the columns, we prepared oriented specimens by drawing fibers from the ϕ_h phase.[1] After cooling to room temperature and annealing for several days at 4 °C, the X-ray fiber diagram yielded significant new information. At room temperature (~25 °C), we observed eight equatorial reflections in the small-angle region that were indexed by a hexagonal lattice with dimension $a = 60.4$ Å. The wide-angle pattern contained two layer lines at an axial repeat of $c = 5.03$ Å. Strong off-meridional maxima are observed on the first layer line at $d = 4.30$ and 3.84 Å, and its was suggested that these could be due to the packing of platelike 3,4,5-tris(benzyloxy)benzoate units that are inclined at 40−50° to the column axis, like the branches of a pine tree. Based on the measured density, the number of monomers contained within a unit cell with dimensions $a = b = 60.4$ Å and $c = 5.03$ Å would be very close to eight. Figure 1 show schematic models with possible 8_1 and 8_4 symmetries, and an 8-fold stacked disk arranagement of monomers consistent with the observed data. The nonstereoregular backbone and the outer regions of the dodecyl tails may have random conformations, and these

* To whom correspondence should be addressed.

® Abstract published in *Advance ACS Abstracts,* February 1, 1995.

0024-9297/95/2228-1552$09.00/0

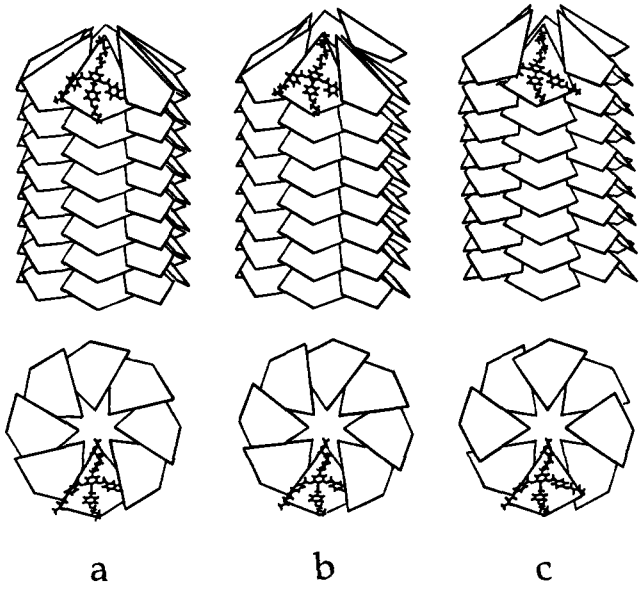

Figure 1. Schematics of possible models for the supramolecular structure of 12-ABG-4EO-PMA in the ordered solid-state form (from ref 1): (a) 8-fold stacked disks; (b) 8_1 symmetry; (c) 8_4 symmetry.

parts of the molecules are omitted from Figure 1 for the sake of clarity.

On heating above the temperature for transition to the ϕ_h phase, the fiber orientation is retained, but there are significant changes in the X-ray data. At 60 °C, six reflections are seen in the small-angle region, which are the first six orders of hexagonal packing on a lattice with a = 58 Å, and indicate a reduction of the column diameter on conversion to the ϕ_h phase. The wide-angle maxima seen for the ordered structure at room temperature also disappear: all that remains is a diffuse halo with very appreciable intensification on the meridian at $d \approx 4.3$ Å. This indicates that the internal order within the columns is much less than that in the ordered phase at room temperature, but some structural correlations remain due to the stacking of the side chains.

The existence of ordered and disordered hexagonal phases has been reported previously for low molecular weight discotic liquid crystals. For example, hexa(hexylthio)triphenylene (HHTT) forms an ordered hexagonal structure in the temperature region 62–70 °C consisting of an array of columns with periodic positional and incommensurate helical intracolumnar order.[8] At 70 °C, there is a transition to a disordered hexagonal phase in which there is only liquidlike ordering of the stacked aromatic cores. It was suggested that the transition corresponds to a disordering of the aliphatic tails. Alkoxyphthalocyaninatopolysiloxanes also form ordered and disordered columnar hexagonal phase.[9]

The present paper follows up on our preliminary investigations of the structure of 12-ABG-4EO-PMA by studying the changes in the X-ray data as the fibers are heated, cooled, and reheated. It will be seen that changes in temperature effect a continuous change on the dimensions and internal structure of the columns and that these changes are accompanied by remarkable changes in the gross dimensions of the fibers.

Experimental Section

The specimens of 12-ABG-4EO-PMA were those used previously,[1] which were synthesized as described by Percec *et al.*[2a] The molecular weights determined by GPC were M_w = 36 000 and M_n = 24 000, corresponding to a number-average degree of polymerization (DP) of ~19. Fibers were drawn with tweezers from the homogeneous film of the polymer on a microscope slide at 60 °C, cooled to room temperature, and stored in the refrigerator at 4 °C for several days.

X-ray patterns were recorded for single fibers on Kodak direct exposure film, using Ni-filtered Cu Kα radiation and pinhole or toroidal collimation. The fiber specimens were mounted vertically and perpendicular to the horizontal X-ray beam. The wide-angle d-spacings were calibrated using calcium fluoride. The heating unit stage used with the specimen holder had an accuracy of approximately ±0.1 °C. Equilibration was achieved within 5 min of heating the stage to the desired temperature in the range of 20–100 °C. The d-spacings were measured from the film data using an Optronics P1000 scanning optical densitometer. The line width for the wide-angle equatorial maximum at d = 4.59 Å was determined from a densitometer scan along the equator. Following subtraction of the "amorphous" background (estimated by eye), the peak at d = 4.59 Å was separated from its two weaker neighbors by curve fitting of Gaussian functions. The apparent crystallite size was determined from the integral half-width using the Scherrer equation.

Small-angle X-ray data were also recorded at room temperature (25 °C) using a Philips PN 3550/10 diffractometer in the transmission mode, with a slit width of 0.033° and Cu Kα radiation. Data were recorded along the equatorial direction for a single oriented fiber. Following subtraction of a weak nonlinear background (estimated by eye), line widths for the 100 (d = 51.8 Å) and 200 (d = 26.2 Å) maxima were estimated as the integral half-widths of fitted Gaussian functions. Measurements on a standard silicon sample indicated that the instrumental broadening was 0.035° in the region of the observed data. The crystallite size for the hexagonal lattice was determined from the integral widths of the 100 and 200 maxima, following correction for instrumental broadening and paracrystalline distortion.[10]

Thermal analysis was performed using a Perkin-Elmer DSC-7 differential scanning calorimeter (DSC), at a scan rate of 20 °C/min. The density of the specimen in the range of 20–60 °C was determined by flotation in DMSO–water mixtures. Changes in the dimensions of the fiber as a function of temperature in the range 20–95 °C were measured using a Carl–Zeiss polarized optical microscope equipped with a Mettler FP82 hot stage.

Results and Discussion

DSC. DSC traces for successive heatings and coolings for oriented fibers of 12-ABG-4EO-PMA are shown in Figure 2. The phase transition temperatures and associated enthalpy changes are given in Table 1. The initial specimen had been annealed at 4 °C for 5 days prior to recording the DSC data. During the first heating scan a, we observed transitions at 42.0 and 95.5 °C, which are assigned as the ordered solid state-to-ϕ_h and the ϕ_h-to-isotropic transitions, respectively. The enthalpy change for the first transition is much greater than that for isotropization. This is consistent with a transition from one state consisting of columns with a structurally ordered interior to one in which the columns have a more liquidlike interior. Transition from the latter structure to the isotropic state should be characterized by a lower enthalpy change. Small differences occurred in the transition temperatures and enthalpies recorded for different specimens: the data in Figure 2 are for the specimen giving the highest transition enthalpies in the first heating scan.

Scans b and c were recorded during cooling and immediate reheating of the above specimen. It can be seen that the isotropic melt is converted to the ϕ_h form on cooling but that there is no re-formation of the ordered solid-state structure on cooling to room temperature. Curve d shows the third heat scan for a

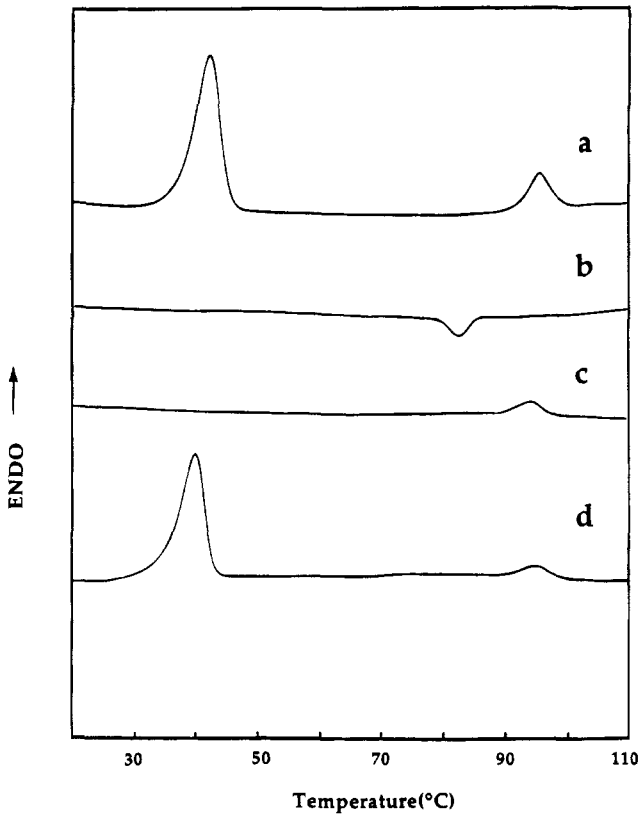

Figure 2. DSC scans of oriented fibers of 12-ABG-4EO-PMA in the range of 20–100 °C: (a) 1st heating scan after annealing for 5 days at 4 °C; (b) 1st cooling; (c) 2nd heating; (d) reheating after specimen c had been cooled and reannealed for 5 days at 4 °C.

Table 1. Phase Transition Temperatures (°C) and Corresponding Enthalpy Changes (in Parentheses, kcal/mru) Determined by DSC for Oriented Fibers of 12-ABG-4EO-PMA[a]

1st heating	k	42.0 (5.60)	ϕ_h	95.5 (1.00)	i
1st cooling			ϕ_h	82.9 (0.44)	i
2nd heating			ϕ_h	94.2 (0.37)	i
3rd heating	k	39.6 (4.46)	ϕ_h	94.7 (0.30)	i

[a] k = ordered solid state; ϕ_h = hexagonal columnar mesophase; i = isotropic phase.

similar specimen after storing in the refrigerator for 5 days at 4 °C. The lower transition is now detected, indicating re-formation of the ordered solid state at room temperature. However, the enthalpy change (4.46 kcal/mru) associated with this transition is less than that observed for the original specimen (5.60 kcal/mru), perhaps due to the fact that the specimen is now unoriented and less well ordered. Generally speaking, the enthalpy for the first transition increased steadily with annealing time and reached a maximum after about 5 days at 4 °C.

Figure 3 shows the first and second heating scans limited to the range 0–60 °C for an oriented specimen. We see the ordered solid state-to-ϕ_h transition in the first heating scan but not in the second, indicating that the ordered solid-state structure is not reformed immediately on cooling the oriented specimen. Curve *c* is the heating scan for a specimen that had been heated up to 60 °C, cooled to 0 °C, and stored in the refrigerator for 5 days at 4 °C. It can be seen that the ordered solid state-to-ϕ_h transition is restored with approximately the same enthalpy change as that for the original fibers.

Small Angle X-ray Diffraction. Figure 4 shows the small-angle X-ray patterns for a single annealed fiber

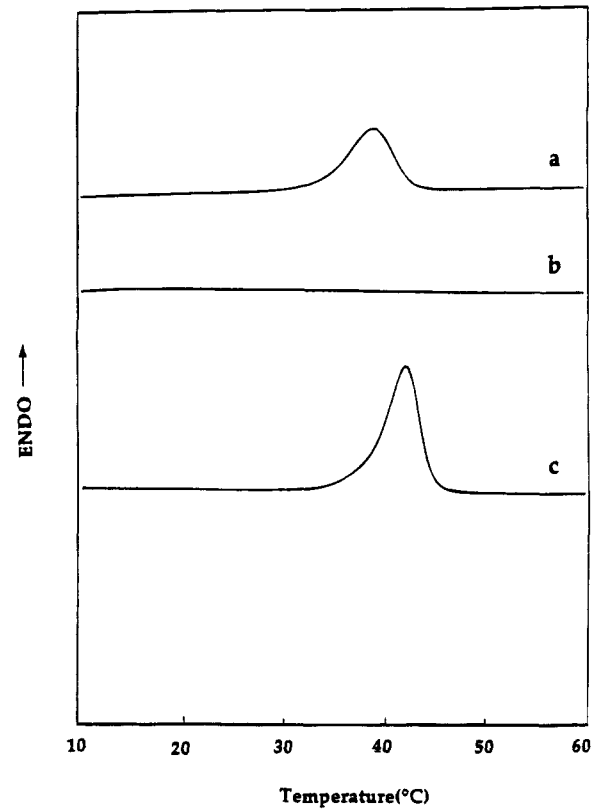

Figure 3. DSC scans for oriented fibers of 12-ABG-4EO-PMA in the range of 0–60 °C: (a) 1st heating after annealing for 5 days at 4 °C; (b) 2nd heating; (c) reheating after specimen b had been cooled and reannealed for 5 days at 4 °C.

of 12-ABG-4EO-PMA recorded on film at 21.4 °C (a) and after heating in successive steps to 58.1 °C (b). The data are for 10-h exposures recorded after equilibrium at the temperature specified. The specimen at 58.1 °C was allowed to cool to room temperature in the X-ray camera (this took approximately 1 h), after which the X-ray data were recorded at 22.0 °C. Finally X-ray data were recorded on heating successively to 39.7, 72.1, and 94.7 °C. The *d*-spacings observed in the small-angle region at each temperature are listed in Table 2. It can be seen that these data vary with temperature. However, at each temperature they are (within experimental error) in the ratio $1:1/\sqrt{3}:1/2:...$, which is characteristic of hexagonal packing. The *a* dimension for the hexagonal lattice was calculated for each temperature of observation on the basis of the best fit for the *d*-spacings of the first three reflections (which can be measured most accurately). These dimensions are also given in Table 2 and are plotted against temperature in Figure 5.

In the first heating experiments, we see an increase in the *a* dimension from 59.8 Å at 21.4 °C to 60.5 Å at 39.9 °C, after which *a* declines to 59.1 Å at 58.1 °C. On cooling to 22.0 °C, *a* increases to 61.1 Å, significantly more than the value of 59.9 Å seen at 21.4 °C for the original specimen. On reheating, *a* decreases to 60.7 Å at 39.7 °C, which is essentially the same as the value of 60.5 Å observed at 39.9 °C in the first heating experiments, and then follows the latter data at higher temperatures. In the second heating experiments, we went to still higher temperatures, close to the ϕ_h-to-isotropic transition. The decline in *a* with temperature becomes steeper at higher temperatures, and there is also a decrease in the degree of orientation as judged by the increased arcing of the small-angle maxima. At 94.7 °C, we observe only a relatively broad diffraction

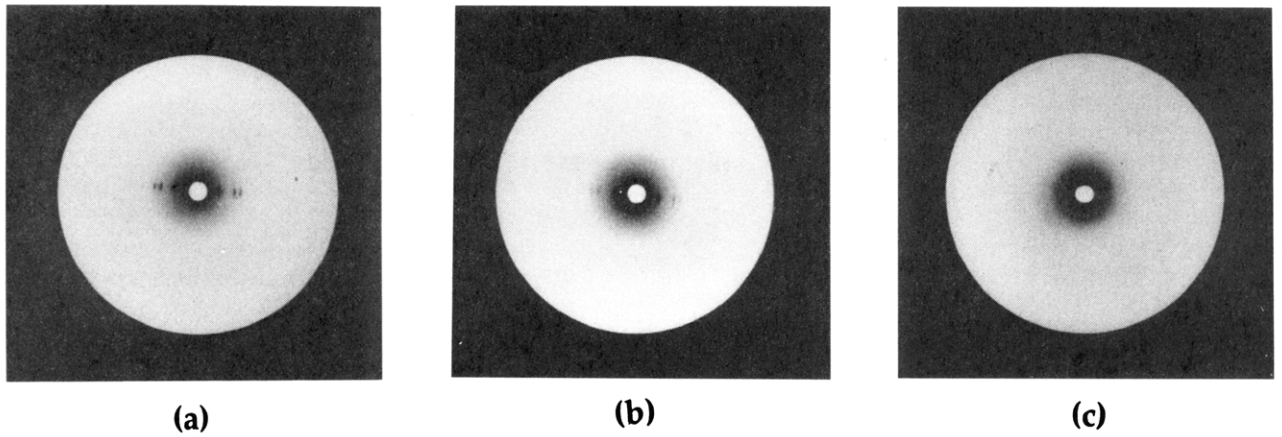

Figure 4. Small-angle X-ray data for an oriented fiber of 12-ABG-4EO-PMA that had been annealed for 5 days at 4 °C. The data were recorded at (a) 21.4 °C, (b) 58.1 °C, in the first heating series, and (c) 94.7 °C in the second heating series.

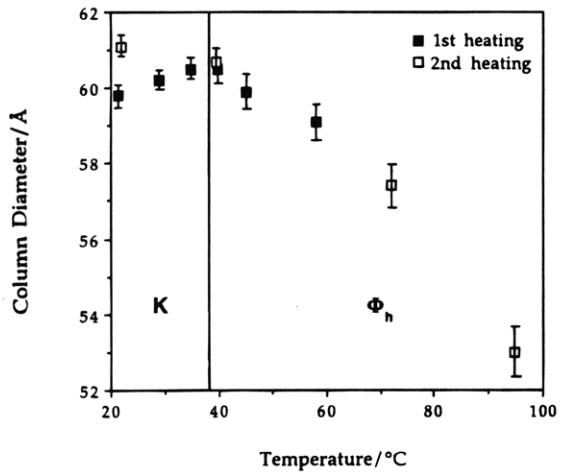

Figure 5. Column diameters at different temperatures determined from the small-angle X-ray data for an oriented fiber of 12-ABG-4EO-PMA: (■) first heating; (□) second heating.

Table 2. Observed *d*-Spacings and Column Diameters (Å) for 12-ABG-4EO-PMA at Different Temperatures

	temp (°C)	*hkl* 100	110	200	210	300	column diameter
1st heating	21.4	51.5	30.0	26.0	19.6	17.3	59.8 ± 0.02
	28.7	52.0	30.1	26.1	19.7	17.4	60.2 ± 0.02
	34.8	52.5	30.1	26.3	19.8	17.5	60.5 ± 0.03
	39.9	52.5	30.1	26.3	19.7		60.5 ± 0.03
	45.2	51.5	30.0	26.1	19.6		59.9 ± 0.03
	58.1	51.0	29.6	25.6	19.4		59.1 ± 0.03
2nd heating	22.0	53.0	30.7	26.5	20.1	17.7	61.1 ± 0.02
	39.7	52.2	30.3	26.3	19.7	18.7	60.7 ± 0.02
	72.1	49.5	28.7	24.9	18.8		57.4 ± 0.03
	94.7	46.0					53.0 ± 0.04

ring at $d = 46$ Å (Figure 4c), which would correspond to a cylinder diameter of $a \approx 54$ Å if packed hexagonally. Above the ϕ_h-to-isotropic transition, there are no small angle maxima.

The change in slope at ~39 °C in the plot of a vs T for the first heating experiment correlates with the ordered solid state-to-ϕ_h phase transition seen in the DSC data. On cooling the specimen from 58.1 to 22.0 °C, a increases steadily to 61.1 Å, consistent with the DSC data that indicate that the ϕ_h form is quenched and an ordered solid-state structure is not reformed. However, in the specimen that had been annealed in the refrigerator for 5 days at 4 °C prior to recording the heating scan (Figure 3c), the a dimension reduced to

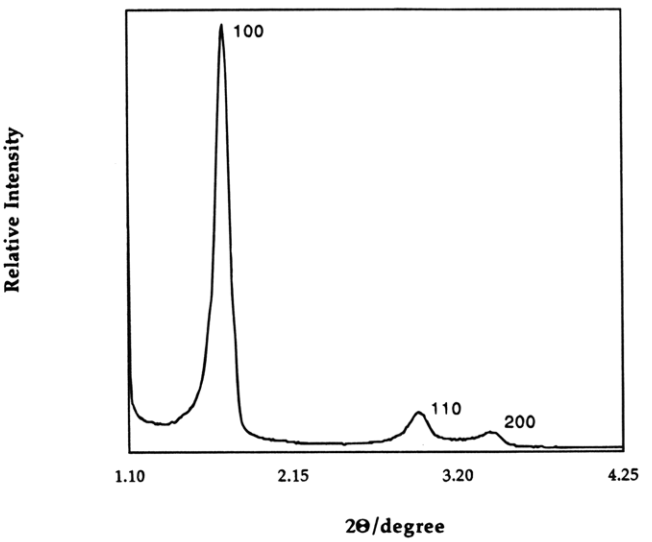

Figure 6. Small-angle equatorial X-ray diffractogram for an oriented annealed fiber of 12-ABG-4EO-PMA at room temperature (~25 °C).

Table 3. *d*-Spacings and Integral Peak Half-Widths for the Small-Angle Equatorial Reflections of Oriented Fibers of 12-ABG-4EO-PMA

d (Å)	integral half-width (deg)
51.8	0.113 ± 0.002
30.0	0.197 ± 0.003
26.0	0.287 ± 0.005

59.8 Å at 21.4 °C, indicating re-formatiion of the ordered solid-state structure.

Figure 6 shows an equatorial diffractometer scan in the small-angle region at room temperature (~25 °C) for a single fiber that had been annealed at 4 °C for 5 days. The observed d-spacings are also listed in Table 3 and are indexed by a hexagonal unit cell with $a = 60.4$ Å, consistent with the other data. The Bragg reflections are very sharp: following subtraction of the diffuse background and fitting Gaussian function, we determined integral half-widths of 0.113 ± 0.002 and 0.287 ± 0.003° for the 100 and 200 reflections. After correction for instrumental broadening (assuming Gaussian profiles), and also for paracrystalline distortion, we obtained a crystallite size of 820 ± 18 Å using the Scherrer equation. (If we assume Lorentzian profiles, the crystallite size obtained is 805 ± 24 Å, which is essentially the same.) Thus there is a high degree of lateral order in the packing of the cylinders, extending

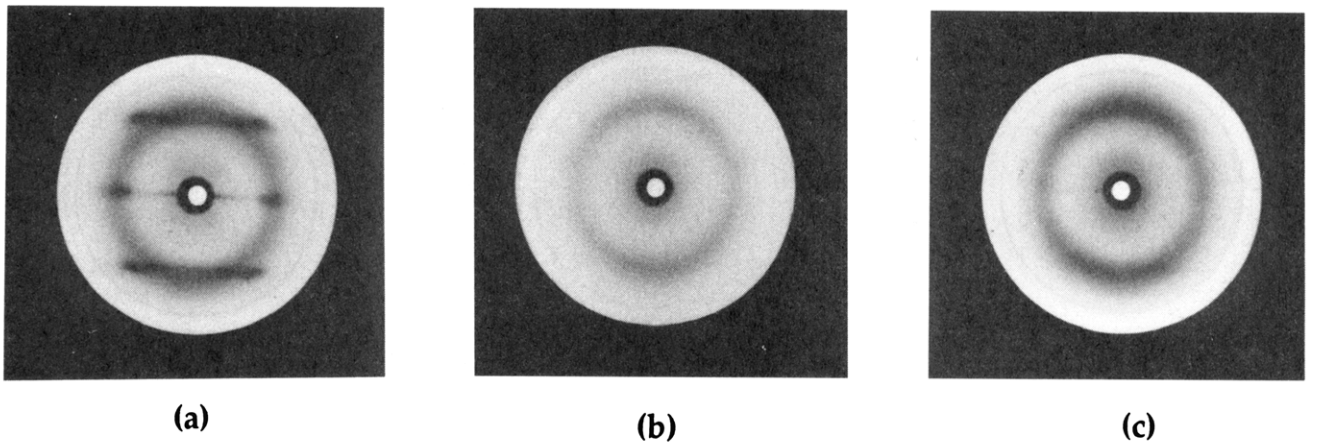

Figure 7. Wide-angle X-ray data for an oriented fiber of 12-ABG-4EO-PMA at (a) 21.4 °C after annealing at 4 °C for 5 days, (b) 39.9 °C (specimen a), and (c) 22.0 °C (specimen b) after it had been heated to 58.1 °C and then cooled.

over at least 13−14 cylinders. The Hoseman paracrystalline g_{II} parameter is ~4%, consistent with the observation of 3 orders of $h00$ reflections. We did not record diffractometer data at higher temperatures, because our temperature control was more reliable for the film data. However, the integral half-widths determined from densitometer scans of the 100 reflection recorded on film indicate a significant increase in the crystallite size after the transition to the ϕ_h phase.

Examination of the 100 peak in Figure 6 shows that the profile is in fact neither Gaussian nor Lorentzian but is distinctly asymmetric. Part of this asymmetry may be due to the use of slit collimation, but this is not the entire explanation, because the observed asymmetry is different from specimen to specimen. This peak may have more than one component, perhaps due to the coexistence of ordered and disordered cylinders with almost but not quite the same diameters. Fontes *et al.*[8] were able to resolve 100 peaks for both the ordered and disordered columnar hexagonal phases for HHTT, which occur at $d = 18.81$ and 18.59 Å, on heating to the region of the phase transition. For our polymer, it is reasonable also to expect a change in column diameter at the phase transition. If this is the case, then the crystallite size for the ordered phase will be higher than 820 Å. Further studies of the peak profiles are now in progress.

The small increases in a from 59.8 Å at 21.4 °C to 60.5 Å at 39.9 °C can be understood in terms of thermal expansion of the ordered structure. The subsequent lateral contraction to 53.0 Å at 94.7 °C points to a major rearrangement of the internal structure of the columns in the ϕ_h phase. A similar lateral contraction was seen for the ϕ_h phase of HHTT,[8] for which the a dimension decreases from 21.49 to 20.97 Å as the temperature increases from 74 to 89 °C. However, the magnitude of the effect is not as large as that in the present structure: the lateral expansion coefficient is -1.6×10^{-3}/deg for HHTT, compared to -2.3×10^{-3}/deg for 12-ABG-4EO-PMA. Sauer[9] has also reported negative lateral thermal expansion for 2,6,11,15-methoxy-3,7,-10,14-octalkoxyphthalocyaninatopolysiloxane (C1C8-PCPS): a decreased from 22.9 to 22.4 Å as the temperature increased from 45 to 115 °C, corresponding to a lateral expansion coefficient of -3.1×10^{-4}/deg.

For both HHTT and C1C8PCPS, it was suggested that the contraction occurred due to thermal melting of the alkoxy tails, which could then be accommodated in a smaller diameter, although this would require an increase in density if the original stacking of the aromatic disks were to be maintained. In the case of 12-ABG-4EO-PMA, there is actually a small decrease in density with increasing temperature in the ϕ_h phase (see below), and hence one cannot explain the closer packing simply by a contraction of the alkyl tails. Rather, the change in column diameter must also involve a reduction in the number of monomers per unit length.

Wide-Angle X-ray Data. Figure 7a shows the wide-angle X-ray pattern recorded at 21.4 °C for an oriented fiber that had been annealed for 5 days at 4 °C. We observe two layer lines at an axial spacing of $c = 5.03$ Å, as reported previously[1] for a specimen at room temperature (~25 °C). The equator and layer lines contain a number of distinct maxima, indicating the existence of three-dimensional order.

The line width of the strong wide-angle equatorial at $d = 4.59$ Å was determined from a densitometer scan of the film data recorded at 21.4 °C, which gave better resolution of three peaks in this region than the diffractometer data. Construction of the "amorphous" background in this region is difficult and a range of options are tried, followed by separation of the three peaks by fitting Gaussian functions. It was concluded that the lateral "crystalline size" based on wide-angle line broadening is not greater than 50 Å. This dimension is less than the lateral until cell dimension and well below the crystalline size of 820 Å determined from the small-angle line widths. Consequently the wide-angle maxima arise primarily from the internal order of the cylinders; i.e., they are peaks in the cylindrically averaged Fourier intensity transform of the individual cylinder, rather than Bragg reflections.

Thus it appears that the ordered solid-state structure contains cylinders which have a well-defined internal structure. These are placed on a highly ordered hexagonal array, but there may be complete freedom for rotation about and displacement along the c axis. Hence, it is more appropriate to describe the annealed structure formed below 39.9 °C as three-dimensionally ordered, rather than crystalline. We envisage a structure in which the main features are determined by the necessity to stack the 3,4,5-tris(benzyloxy)benzoate units, but in which there is probably randomness in the backbones, and in the parts of the dodecyl and tetraethoxy groups away from the aromatic units. In any case, a disordered conformation is to be expected for the backbones, which are not stereoregular.

Table 4. Wide-Angle Data for 12-ABG-4EO-PMA along the Fiber Axis Direction

	temp (°C)	fiber repeat (Å)	*d*-spacing of meridional arc (Å)
1st heating	21.4	5.01 ± 0.02	
	28.7	4.99 ± 0.02	
	39.9		4.35 ± 0.05
	45.3		4.40 ± 0.05
	58.1		4.50 ± 0.05
	75.2		4.50 ± 0.05
	87.1		4.60 ± 0.05
1st cooling	22.0	5.00 ± 0.05	4.35 ± 0.05

The strongest wide-angle maxima are at $d = 4.30$ and 3.84 Å on the first layer line, and we have suggested previously[1] that these arise due to an inclination of relatively extended monomer units relative to the fiber axis. The maximum at $d = 4.30$ Å may also relate to ordering of the inner regions of the dodecyl tails: note that a $hk0$ reflection with $d = 4.23$ Å is seen for the hexagonal form of polyethylene.[11] Randomness in the outer regions of the dodecyl tails would preclude three-dimensional correlations beyond hexagonal packing. Futher work is in progress to define the internal structure of the cylinders in more detail.

Table 4 summarizes the wide-angle data for 12-ABG-4EO-PMA along the fiber axis direction of different temperatures for the first heating series and subsequent cooling. The data at 21.4 and 28.7 °C are essentially the same, and we observe the same fiber repeat within experimental error. On heating to 39.9 °C, the wide-angle pattern (Figure 7b) changes to that characteristic of the oriented ϕ_h phase. We see a diffuse meridional intensity at $d = 4.35$ Å, suggesting that the "planes" of the monomer units now have preferential orientation perpendicular to the *c*-axis, although in view of the arcing of this maximum there is a broad distribution about the preferred position. It appears that otherwise the internal structure of the column is liquidlike; i.e., there is no regular disklike or helical stacking. Since the cylinder diameter declines at the ordered solid state-to-ϕ_h transition, there is mostly likely a contraction of the tetraethoxy spacer and/or the $CH_3(CH_2)_{11}$ tails. The results are consistent with a relatively extended conformation for the tilted arms of the "pine tree" in the ordered solid-state structure, which become shorter with the introduction of more *gauche* conformations when disordered in the ϕ_h phase.

On increasing the temperature from 39.9 to 87.1 °C, the gross features of the wide-angle pattern are unchanged, but the meridional maximum broadens along the fiber axis direction and shifts to higher *d*-spacings. These data point to a more disordered stacking of the monomer units, with a small increase in their separation. There is also progressive loss in orientation as the temperature is increased above 60 °C. Figure 7c shows the wide-angle pattern recorded after cooling from 58.1 to 22.0 °C. These data are largely the same as those obtained at 39.9 °C, again suggesting that we have retained (i.e., quenched) the ϕ_h structure. However, on closer inspection of the data, we see traces of a layer line at $d \approx 5.0$ Å, indicating that there has been reformation of a very small amount of the ordered solid-state structure. Annealing in the refrigerator at 4 °C for 5 days strengthens this layer line and also restores the other features of the original pattern, such that the data become indistinguishable from those for Figure 7a.

Measurement of Fiber Dimensions and Density. The changes in the gross dimensions of the fiber as a function of temperature were followed by optical microscopy. Figure 8 shows micrographs of a typical fiber sample at 25 and 95 °C, where we see a striking increase in length of ~28% and a decrease in width of ~14% at the higher temperature. Figure 9 shows a plot of fiber dimensions versus temperature during, heating in this temperature range. The length stays approximately constant before the transition to the ϕ_h phase; there is an appreciable increase in length at the transition, after which the length increases in an almost linear manner. Figure 9 also shows the change in width for the same specimen, which is approximately constant up to ~40 °C and then decreases steadily in the ϕ_h phase. By and large the percentage decrease in width parallels and is approximately half the increase in length. Density

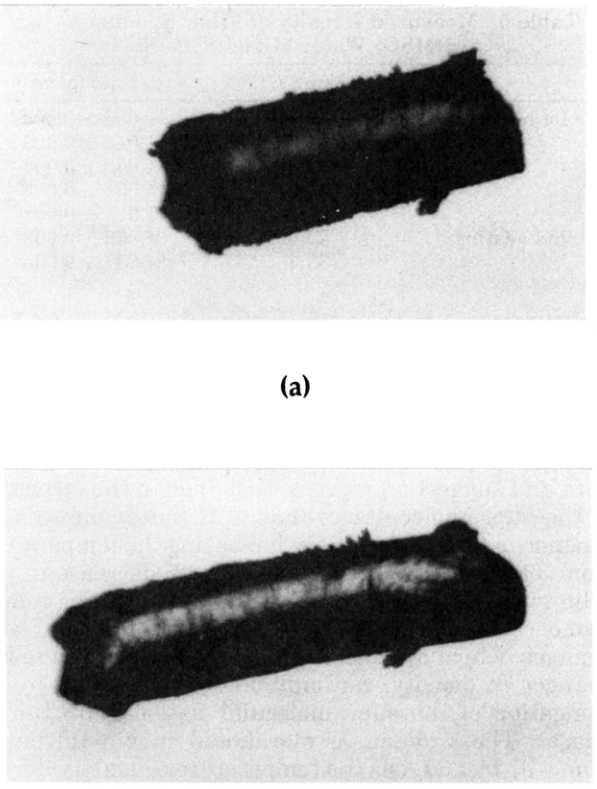

Figure 8. Optical micrographs of an oriented fiber of 12-ABG-4EO-PMA at (a) 25 and (b) 95 °C.

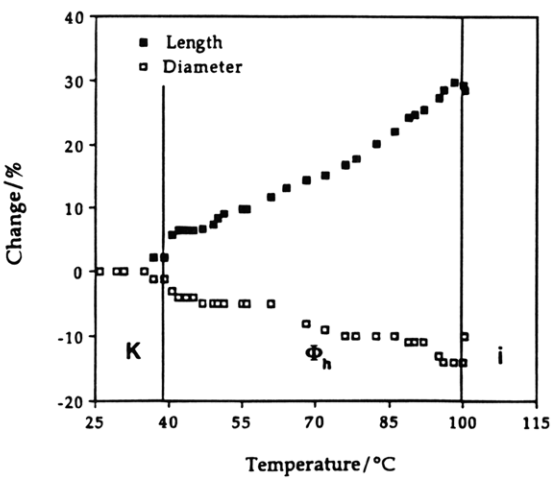

Figure 9. Plot of fiber dimensions as a function of temperature: (■) length; (□) diameter. The positions of the ordered solid state (K)-to-columnar hexagonal phase (ϕ_h) transition and ϕ_h-to-isotropic (i) transition are isolated by the vertical lines.

Table 5. Measured Density of Fiber Specimens in a DMSO–Water Mixed Solvent

	temp (°C)	density (g/cm³)
1st heating	21.4	1.055 ± 0.003
	28.7	1.046 ± 0.003
	34.8	1.042 ± 0.004
	45.3	1.034 ± 0.005
	58.1	1.011 ± 0.008
2nd heating	22.0	1.056 ± 0.003
	39.7	1.037 ± 0.005

measurements in the temperature range 21.4–58.1 °C are presented in Table 5: we see a 4% decrease in density over this range, in which there is ~10% increase in length and a ~5% decrease in width.

The changes in the fiber morphology correlate with the observed changes in the small- and wide-angle X-ray data and suggest a progressive change in the structure of the supramolecular cylinders in the ϕ_h phase as a function of temperature. On increasing the temperature from 39.9 to 94.7 °C, there is a 12.4% decrease in the column diameter, which compares well with the reduction of ~14% in the observed width of the fiber. These changes, which are also in the opposite direction to the changes in density, can only be accommodated by an elongation of the supramolecular assembly in the ϕ_h phase. The wide-angle meridional maximum shifts from 4.35 to 4.60 Å as the temperature is increased from 39.9 to 87.1 °C, pointing to an increased separation between the stacked aromatic units. However, this 5% change could not account for the approximately 23% change in length over the same temperature range.

Consequently, there must be a substantial change in the supramolecular assembly in the ϕ_h phase, such as a partial unwinding of a distorted helical conformation, leading to a progressive reduction in the number of monomers per unit length. The reason for such a change in the conformation within the cylinder might reside in the interactions between the tapered side chains with temperature. It is also possible that the poly(methacrylate) backbone in ordered structure has a less than ideal contracted conformation but that this is compensated by the favorable stacking of the side chains. At the transition to the ϕ_h phase, there is a change in the latter interactions, whereupon the backbone may be free to adopt a somewhat more extended conformation, leading to a reduction in the number of monomers per unit length and in the column diameter.

Conclusions

At room temperature, 12-ABG-4EO-PMA adopts an ordered solid-state structure in which supramolecular cylindrical moieties are packed on a hexagonal lattice. The internal structure of the cylinders consists of approximately eight monomers arranged with the planes of the side chains tilted and/or twisted by 40–50° from the plane perpendicular to the fiber axis. There is no evidence for lateral or axial structural correlations between adjacent columnar units, other than the hexagonal packing, which extends over dimensions ≥820 Å. Hence, the outer regions of the dodecyl tails may have random conformations. When the room temperature structure is heated, the internal order in the cylinder is largely unaffected before we reach the transition to the ϕ_h phase, but there is a small increase in the cylinder diameter, which parallels the small decrease in density. At the ordered solid state-to-ϕ_h transition, the internal structure becomes liquidlike, such that the only structural correlations are due to relatively disordered stacking of the side chains, which are now inclined more nearly perpendicular to the fiber axis. The disorder probably reflects the thermal motions characteristic of a liquid crystalline state. An elongation of the backbone conformation may allow a drawing in and reorientation of the aromatic units, leading to a reduction in the cylinder diameter. As the temperature rises there is a continued decrease in the diameter of the cylinder, and at the same time there is an increase in the axial separation of the side chains.

On cooling to room temperature, the structure characteristic of the ϕ_h phase is quenched, and the column diameter now exceeds that for the ordered solid-state structure. However, a trace of the latter structure can be detected, and the original level of ordering is restored on annealing at 4 °C for about 5 days. The structural changes with temperature in the ϕ_h phase are paralleled by very striking changes in the dimension of the specimen of the oriented fiber and suggest a progressive change in the number of monomers per unit length within the supramolecular cylindrical moieties.

Acknowledgment. This work was supported by NSF Materials Research Grant DMR 91-22227 on Liquid Crystalline Polymers.

References and Notes

(1) Kwon, Y. K.; Chvalun, S.; Schneider, A.-I.; Blackwell, J.; Percec, V.; Heck, J.-A. *Macromolecules* **1994**, *27*, 6129.
(2) (a) Percec, V.; Heck, J.; Tomazos, D.; Falkenberg, F.; Blackwell, H.; Ungar, G. *J. Chem. Soc., Perkin Trans. 1* **1993**, 2799. (b) For a brief review, see: Percec, V.; Heck, J.; Johansson, G.; Tomazos, D. *Makromol. Symp.* **1994**, *77*, 237. (c) Percec, V.; Heck, J.; Ungar, G. *Macromolecules* **1991**, *24*, 4957.
(3) (a) Klug, A. *Harvey Lect.* **1979**, *74*, 141. (b) Klug, A. *Angew. Chem., Int. Ed. Engl.* **1993**, *22*, 565.
(4) For some reviews and recent papers on phasmidic, rod-shaped, disk-shaped, cone-shaped, and diabolo-like liquid crystals constructed with 12-ABG and other related molecules, see: (a) Malthête, J.; Collet, A.; Levelut, A. M. *Liq. Cryst.* **1989**, *5*, 123. (b) Gasparoux, H.; Hardouin, F.; Destrade, C.; Nguyen, H. T. *New J. Chem.* **1992**, *16*, 292. (c) Malthête, J.; Nguyen, H. T.; Destrade, C. *Liq. Cryst.* **1993**, *13*, 171. (d) Malthête, J.; Levelut, A. M. *Adv. Mater.* **1991**, *3*, 94. (e) Xu, B.; Swager, T. M. *J. Am. Chem. Soc.* **1993**, *115*, 1159. (f) Serrette, A. G.; Swager, T. M. *J. Am. Chem. Soc.* **1993**, *115*, 8879.
(5) (a) Ebert, M.; Kleppinger, R.; Soliman, M.; Wolf, M.; Wendroff, J. H.; Lattermann, G.; Staufer, G. *Liq. Cryst.* **1990**, *7*, 553. (b) Festag, R.; Kleppinger, R.; Soliman, M.; Wendorff, J. H.; Lattermann, G.; Staufer, G. *Liq. Cryst.* **1992**, *11*, 699.
(6) (a) Brienne, M.-J.; Gabard, J.; Lehn, J.-M.; Stibor, I. *J. Chem. Soc., Chem. Commun.* **1989**, 1868. (b) Fouquey, C.; Lehn, J.-M.; Levelut, A.-M. *Adv. Mater.* **1990**, *2*, 254. (c) Krzywicki, T. G.; Fouquey, C.; Lehn, J.-M. *Proc. Natl. Acad. Sci. U.S.A.* **1993**, *90*, 163. (d) For a review, see: Lehn, J.-M. *Makromol. Chem., Macromol. Symp.* **1993**, *69*, 1.
(7) (a) Chandrasekhar, S. *Liq. Cryst.* **1993**, *14*, 3. (b) Chandrasekhar, S.; Ranganath, G. S. *Rep. Prog. Phys.* **1990**, *53*, 57. (c) Ungar, G. *Polymer* **1993**, *34*, 2050.
(8) Fontes, E.; Heiney, P. A.; de Jeu, W. H. *Phys. Rev. Lett.* **1988**, *61*, 1202.
(9) Sauer, T. *Macromolecules* **1993**, *26*, 2057.
(10) Bonart, R.; Hosemann, R. *Kolloid Z. Z. Polym.* **1962**, *186*, 16.
(11) Bassett, D. C.; Block, S.; Piermarini, G. J. *J. Appl. Phys.* **1974**, *45*, 4146.

MA941293H